Wave Energy Absorption by Submerged Flap-type Oscillating Wave Surge Converters

CONFERENCE PAPER · SEPTEMBER 2015

READS
16

2 AUTHORS, INCLUDING:

Imogen Noad
University of Bristol
3 PUBLICATIONS **2** CITATIONS

SEE PROFILE

Wave Energy Absorption by Submerged Flap-type Oscillating Wave Surge Converters

Imogen Noad
School of Mathematics, University of Bristol
University Walk, Bristol, BS8 1TW, UK
E-mail: imogen.noad@bristol.ac.uk

Richard Porter
School of Mathematics, University of Bristol
University Walk, Bristol, BS8 1TW, UK
E-mail: richard.porter@bristol.ac.uk

***Abstract*—This paper concerns the modelling of the wave energy absorption qualities of three-dimensional, hinged flap-type wave energy converters. An analytical approach is taken to solving a set of boundary value problems arising from the linear water wave problem describing the interaction of the flap converter with the waves. A novel integral formulation and numerical solution is presented, the flexibility and numerical efficiency of which allows us to assess the optimal configuration of such a device. In doing this we consider the impact of varying a range of parameters associated with the device on its wave energy absorption potential, most notably the hinge position, flap length and submersion depth of the device.**

***Index Terms*—Hydrodynamic, flap-type, wave surge converter, optimisation.**

I. Introduction

We use a mathematical approach to consider a variety of aspects concerned with the operation of hinged flap-type wave energy converters. We consider a thin, flat rectangular flap mounted on the sea bed in water of constant, finite depth. This is hinged about a horizontal pivot, below which it is held fixed and above which it is buoyant and free to oscillate. Both the Oyster device of Aquamarine Power Ltd (see [1], [2], for example) and a fully submerged flap are considered. The latter proposal is not currently in testing or manufacture. Complete submersion could be advantageous for many reasons, not least the increased survivability afforded by complete submersion. The purpose of this paper is to compare the behaviour of the two device types: to weigh up their relative potentials for wave power absorption and to consider the impact on the hydrodynamic effects of full submersion.

Much of the development work on Oyster has been carried out using numerical CFD and experimental wave tank testing [2], [3]. However, a recent paper [4] has approached the hinged flap-type problem. Our paper uses the same background theory as contained therein, however there are key differences in the mathematical solution method to the hydrodynamic problems that arise. In our approach we exploit the geometry to apply Fourier transforms, leading to non-singular integral equations in terms of unknown functions relating to the pressure jump across the flap. These are solved numerically using a highly efficient Galerkin expansion method resulting in a low-order system of equations. In contrast [4] use Green's functions to develop hypersingular integral equations, solved by collocation. The problem of a fully submerged device necessitates a significant extension of the mathematical approach used in [5] for an array of surface-piercing flap-type devices.

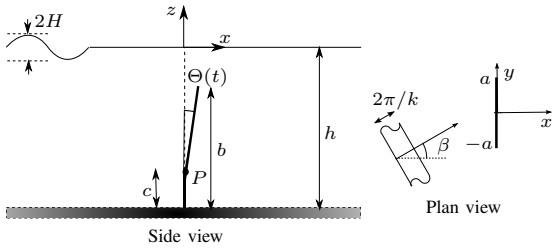

Figure 1. The flap converter used in the hydrodynamic model.

We then exploit the numerical efficiency of the solution to perform an optimisation over a number of free parameters associated with the theoretical problem. This allows us to assess the optimal configuration of a surface-piercing flap-type device similar to the Oyster under a realistic random sea state. In particular, it is demonstrated that the length of the flap is critical to its performance. Further, parameters associated with a submerged flap are considered; the effect of the submersion depth and device length on performance being analysed.

II. Formulation

Cartesian coordinates have been chosen with the origin at the mean free surface level and z pointing vertically upwards. The fluid has density ρ and is of constant, finite depth h. The hydrodynamic model assumes the flap to be infinitely thin and buoyant so that when at rest it occupies the vertical plane $\{x = 0, -a < y < a, -h < z < -h + b\}$, where $b < h$. It is hinged along a horizontal axis $(x, z) = (0, -h + c)$, which is denoted in figure 1 by P. Above its pivot the flap is free to move and below it is held fixed and vertical. The fluid is incompressible and inviscid, the flow is irrotational and the flap oscillations are assumed to be of small amplitude. A standard linearised theory of water waves is used.

Small amplitude plane waves of radian frequency ω are incident from $x < 0$, making an anti-clockwise angle $\beta \in (-\pi/2, \pi/2)$ with the positive x-direction.

After removing the harmonic time-dependence, the velocity potential is decomposed as

$$\phi(x, y, z) = A\phi^S(x, y, z) + \Omega\phi^R(x, y, z) \qquad (1)$$

where Ω is the complex angular velocity, $A = igH/2\omega\psi_0(0)$ ensures an incident wave height H and ψ_0 is a normalised depth eigenfunction which will be defined later. Here ϕ^S and ϕ^R are associated with the scattered and radiated wave fields respectively. They satisfy

$$\bigtriangledown^2\phi^{S,R} = 0 \tag{2}$$

in the fluid,

$$\phi_z^{S,R} - \frac{\omega^2}{g}\phi^{S,R} = 0 \tag{3}$$

on $z = 0$, and

$$\phi_z^S = 0 \qquad \text{and} \qquad \phi_z^R = 0 \tag{4}$$

on $z = -h$. Further, we have

$$\phi_x^S\left(0^{\pm}, z\right) = 0 \qquad \text{and} \qquad \phi_x^R\left(0^{\pm}, z\right) \quad = u(z) \tag{5}$$

for $-a < y < a$ and $-h < z < -h + b$, where

$$u(z) = \begin{cases} 0, & z \in [-h, -h + c] \cup [-h + b, 0] \\ z + h - c, & z \in [-h + c, -h + b]. \end{cases} \tag{6}$$

Here, for the surface piercing flap we take $b = h$ whilst for the fully submerged flap we enforce $b < h$.

The incident wave is given by

$$\phi^I(x, y, z) = e^{ik(x\cos\beta + y\sin\beta)}\psi_0(z) \tag{7}$$

where k satisfies $\omega^2 = gk$ tanh kh and $\psi_0(z)$ is a normalised depth eigenfunction defined by

$$\psi_0(z) = N_0^{-1/2}\cosh\, k(z + h), \tag{8}$$

with $N_0 = \frac{1}{2}(1 + \sinh(2kh)/(2kh))$. The potentials ϕ^R and $\phi^D \equiv \phi^S - \phi^I$ describe outgoing waves at large distances from the flap.

In the frequency domain, the equation of motion of the flap is

$$-i\omega I\Omega = -\frac{iC}{\omega}\Omega + F_w + F_e \tag{9}$$

where I denotes the moment of inertia and C the restoring moment, quantities determined by the physical properties of the flap. F_w is the time-independent wave torque and is written as

$$F_w = AF_S + \Omega F_R \tag{10}$$

where

$$F_{S,R} = -i\omega\rho\int_{-a}^{a}\int_{-h}^{0} P^{S,R}(y, z)u(z)\, dz\, dy \tag{11}$$

and

$$P^{S,R}(y, z) = \phi^{S,R}\left(0^+, y, z\right) - \phi^{S,R}\left(0^-, y, z\right) \tag{12}$$

is the pressure difference across $x = 0$. Further decomposition of the radiation force F_R yields

$$F_w = AF_S + (i\omega\mathcal{A} - \mathcal{B})\Omega \tag{13}$$

where the real quantities $\mathcal{A}(\omega)$ and $\mathcal{B}(\omega)$ are the added mass and radiation damping coefficients. Finally, we decide the mechanism for power take-off should take the form of a linear damping force and write

$$F_e = -\lambda\Omega \tag{14}$$

where λ is assumed to be a real constant so that the power and velocity are in phase. It may then be shown (e.g. [6]) that the capture factor can be written as

$$\hat{l} = \frac{W}{2aW_{inc}} = \hat{l}_{max}\frac{2\mathcal{B}}{\mathcal{B} + |Z|}\left(1 - \frac{(\lambda - |Z|)^2}{|\lambda + Z|^2}\right) \tag{15}$$

where W is the time-averaged power absorbed and W_{inc} the power available per unit crest length of incident wave. Further,

$$\hat{l}_{max} = \frac{1}{2a}\frac{|AF_S|^2}{8\mathcal{B}W_{inc}} \tag{16}$$

is the maximum capture factor, achieved through optimal tuning ($\lambda = |Z|$) at resonance ($|Z| = \mathcal{B}$), W_{inc} is the power per unit width of incident wave and

$$Z = \mathcal{B} - i\omega\left(\mathcal{A} + I - \frac{1}{\omega^2}C\right). \tag{17}$$

Further, the optimal capture factor is given by

$$\hat{l}_{opt} = \frac{2\mathcal{B}}{\mathcal{B} + |Z|}\hat{l}_{max} \tag{18}$$

and is achieved through optimal tuning.

Thus, in order to study the performance of the device we must first determine the hydrodynamic coefficients $\mathcal{A}$ and $\mathcal{B}$ along with the exciting force F_S. These depend on the solution of the hydrodynamic problems for ϕ^S and ϕ^R and that is where our attention turns now.

III. Solution of the Hydrodynamic Problems for the Fully Submerged Flap

A. The Scattering Problem

The scattering problem deals with the diffraction of the incident wave when the flap is held fixed vertically. We consider the potential $\phi^D \equiv \phi^S - \phi^I$ associated with the diffracted waves. By antisymmetry we have $\phi^D(x, y, z) = -\phi^D(-x, y, z)$ and so we only need the solution in $x > 0$. We define the Fourier transform of $\phi^D(x, y, z)$ by

$$\overline{\phi}^D(x, l, z) = \int_{-\infty}^{\infty}\phi^D(x, y, z)e^{-ily}\, dy. \tag{19}$$

Then, taking Fourier transforms with respect to y of the governing Laplace equation (2) gives

$$\left(\bigtriangledown_{xz}^2 - l^2\right)\overline{\phi}^D = 0. \tag{20}$$

The most general solution of (20) which also satisfies (3) and (4) with the correct outgoing wave behaviour is

$$\overline{\phi}^D(x, z) = \sum_{r=0}^{\infty} B_r(l)e^{-\lambda_r x}\psi_r(z) \tag{21}$$

where $B_r(l)$ are unknown coefficients,

$$\psi_r(z) = N_r^{-1/2}\cos k_r(z+h), \tag{22}$$

$N_r = \frac{1}{2}(1+\sin(2k_rh)/(2k_rh))$ and k_r are the positive roots of $\omega^2 = -gk_r\tan k_rh$ for $r = 1, 2, ...$ This is consistent with the definition of $\psi_0(z)$ if we let $k_0 = -ik$ and the functions $\psi_r(z)$ for $r = 0, 1, 2, ...$ form a complete set of normalised depth eigenfunctions. Further,

$$\lambda_r(l,k_r) = \begin{cases} \left(k_r^2+l^2\right)^{1/2}, & \text{for } r = 1,2,... \\ \left(l^2-k^2\right)^{1/2}, & \text{for } r = 0 \text{ and } |l| \geq k \\ -i\left(k^2-l^2\right)^{1/2}, & \text{for } r = 0 \text{ and } |l| < k \end{cases}$$

where the choice of branch for λ_0 ensures the radiation condition is satisfied.

We formulate the problem in terms of the unknown pressure difference across the flap, defined in (12). Taking Fourier transforms and using the orthogonality of the depth eigenfunctions we gain the following equations for the unknown coefficients

$$\begin{aligned} B_r(l) &= \frac{1}{2h}\int_{-h}^{-h+b} \overline{P}^S(l,z')\psi_r(z')dz' \\ &\equiv \frac{1}{2h}\int_{-h}^{-h+b}\int_{-a}^{a} P^S(y',z')\psi_r(z')e^{-ily'}dy'\,dz' \end{aligned} \tag{23}$$

for $r = 0, 1, 2, ...$

Invoking the inverse Fourier transform of (21) results in an integral representation for $\phi^D(x,y,z)$

$$\phi^D(x,y,z) = \frac{1}{2\pi}\int_{-\infty}^{\infty}\sum_{r=0}^{\infty} B_r(l)\,e^{-\lambda_r x}\psi_r(z)\,e^{ily}\,dl \tag{24}$$

where $B_r(l)$ for $r = 0, 1, 2, ...$ are expressed in terms of $P^S(y', z')$ in (23). Applying the condition on the flap,

$$\frac{\partial\phi^D}{\partial x}(0^{\pm},y,z) = -\frac{\partial\phi^I}{\partial x}(0^{\pm},y,z) \tag{25}$$

for $-a < y < a$ and $-h < z < -h+b$, then results in an integral equation for $P^S(y,z)$. This may not be solved analytically; instead we employ a Galerkin expansion method. We incorporate the known square-root end-point behaviour through the approximation

$$P^S(y,z) \simeq \sum_{n=0}^{2N+1}\sum_{p=0}^{P}\alpha_{np}w_n(y)\tau_p(z) \tag{26}$$

where

$$w_n(y) = \frac{e^{in\pi/2}}{a(n+1)}\sqrt{a^2-y^2}U_n\left(\frac{y}{a}\right) \tag{27}$$

and

$$\tau_p(z) = \frac{2e^{ip\pi}}{\pi b(2p+1)}\sqrt{b^2-(z+h)^2}U_{2p}\left(\frac{z+h}{b}\right) \tag{28}$$

and $U_n(\cos\theta) = \sin((n+1)\theta)/\sin\theta$ are Chebyshev polynomials of the second kind. Substituting for $P^S(y',z')$ in the integral equation, multiplying through by $-(1/\pi)w_m^*(y)\tau_q(z)$ and integrating over $-a < y < a$, $-h < z < -h+b$ results in the following system of linear equations

$$\sum_{n=0}^{2N+1}\sum_{p=0}^{P}\alpha_{np}M_{npmq} = D_m(\beta)G_{q0} \tag{29}$$

for $m = 0, ..., 2N+1$ and $q = 0, ..., P$, where

$$M_{npmq} = \sum_{r=0}^{\infty} G_{pr}G_{qr}K_{nm}^{(r)} \tag{30}$$

with

$$K_{nm}^{(r)} = \frac{1}{4}\int_{-\infty}^{\infty}\frac{\lambda_r(l,k_r)}{l^2}J_{n+1}(al)J_{m+1}(al)\,dl \tag{31}$$

and

$$G_{pr} = \begin{cases} N_r^{-1/2}J_{2p+1}(k_rb)/k_rh & \text{for } r \geq 1 \\ (-1)^pN_0^{-1/2}I_{2p+1}(kb)/kh & \text{for } r = 0 \end{cases} \tag{32}$$

and

$$D_m(\beta) = \begin{cases} -i\cot\beta J_{m+1}(ka\sin\beta) & \text{if } \beta \neq 0 \\ -\frac{1}{2}ika\delta_{m0} & \text{if } \beta = 0. \end{cases} \tag{33}$$

The integrals which determine $K_{nm}^{(r)}$ vanish when $n+m$ is odd, a rendundancy which allows us to reduce our consideration to elements for which $n+m$ is even. In order to ensure rapid convergence we use an integral result involving products of Bessel functions (Gradshteyn & Ryzhik (1981) §6.538(2)) to gain an integrand which decays like $O\left((ka)^2/l^4\right)$. Ultimately (29) then reduces to a coupled pair of systems which may be solved for the unknown expansion coefficients α_{np}.

The exciting torque on the flap may be expressed in terms of the Galerkin expansion coefficients as

$$F_S = \frac{1}{2}i\omega\rho ah^2\pi\sum_{p=0}^{P}\alpha_{0p}\hat{g}_p \tag{34}$$

where

$$\hat{g}_p = -\int_{-h}^{0}\tau_p(z)u(z)dz, \tag{35}$$

an integral which may be expressed in closed form.

B. The Radiation Problem

Applying the same solution method to the radiation problem, this time making the approximation

$$P^R(y,z) \simeq ah\sum_{n=0}^{2N+1}\sum_{p=0}^{P}\beta_{np}w_n(y)\tau_p(z) \tag{36}$$

for the unknown pressure difference across the flap, results in the following system of linear equations

$$\sum_{n=0}^{2N+1}\sum_{p=0}^{P}\beta_{np}M_{npmq} = E_m\hat{g}_q \tag{37}$$

for $m = 0, ..., 2N+1$ and $q = 0, ..., P$. Here M_{npmq} is defined identically to before,

$$E_m = \frac{1}{2}\delta_{m0} \tag{38}$$

and $\hat{g}_q$ is given in (35).

More rapid convergence of the integrals defining $K_{nm}^{(r)}$ may be achieved as before. Ultimately, having solved for the unknown expansion coefficients β_{np}, we find that the radiation torque is given by

$$F_R = -\frac{1}{2} i\omega\rho a^2 h^3 \pi \sum_{p=0}^{P} \beta_{0p}\hat{g}_p. \tag{39}$$

IV. Solution of the Hydrodynamic Problems for the Surface Piercing Flap

This is a somewhat simpler problem than the fully submerged case since the linearised kinematic condition on the flap (5) now extends throughout the entire depth. It is convenient to expand the forcing $u(z)$ in terms of the complete set of depth eigenfunctions in this case. Thus, we write

$$u(z) = \frac{1}{h}\sum_{r=0}^{\infty} U_r \psi_r(z), \tag{40}$$

where

$$U_r = \frac{N_r^{-1/2}}{k_r^2}\left(k_r(b-c)\sin(k_r b) + \cos(k_r b) - \cos(k_r c)\right) \tag{41}$$

for $r = 0, 1, 2, ...$

A. The Scattering Problem

Since the flap now extends uniformly throughout the entire depth, remaining in a fixed vertical position the depth dependence is now known. Thus, returning to (26) we now write

$$P^S(y,z) \simeq \psi_0(z) \sum_{n=0}^{2N+1} \alpha_n w_n(y) \tag{42}$$

where $w_n(y)$ is defined in (27). Substituting for $P^S(y', z')$ in the integral equation derived in $\S IIIA$, multiplying through by $-(1/\pi)w_m^*(y)\psi_0(z)$ and integrating over $-a < y < a$, $-h < z < 0$ results in the following system of linear equations

$$\sum_{n=0}^{2N+1} \alpha_n K_{nm}^{(0)} = D_m(\beta) \tag{43}$$

for $m = 0, ..., 2N+1$, where $K_{nm}^{(0)}$ and $D_m(\beta)$ were defined in (31) and (33) respectively.

The exciting torque on the flap may be expressed in terms of the Galerkin expansion coefficients as

$$F_S = -\frac{1}{2} i\omega\rho U_0 a h^2 \pi \alpha_0 \tag{44}$$

where U_0 is defined in (41) and is a full depth analogy to $\hat{g}_p$ which arises from the Galerkin expansion through the depth.

B. The Radiation Problem

For the wave radiation problem we use (5) and (40) to write

$$\phi_x^R(0^{\pm}, y, z) = \sum_{r=0}^{\infty} U_r \psi_r(z). \tag{45}$$

So the depth dependence of the pressure jump may be expressed as a superposition of these depth modes and we write

$$P^R(y,z) \simeq ah \sum_{r=0}^{\infty} U_r \psi_r(z) \sum_{n=0}^{2N+1} \beta_n^{(r)} w_n(y) \tag{46}$$

for the unknown pressure difference across the flap in place of (36). This results in the following system of linear equations

$$\sum_{n=0}^{2N+1} \beta_n^{(r)} K_{nm}^{(r)} = \delta_{m0} \tag{47}$$

for $m = 0, ..., 2N+1$ and $r = 0, 1, 2, ...$

Ultimately, having solved for the unknown expansion coefficients $\beta_n^{(r)}$, we find that the radiation torque is given by

$$F_R = -i\omega\rho a^2 h\pi \sum_{r=0}^{\infty} U_r^2 \beta_0^{(r)}. \tag{48}$$

V. Numerical Calculations

A. Angle of Excursion

The formulation is based on a linearised theory of water waves and there has been an *a priori* assumption that excursions of the flap from the vertical are small in order that the results retain validity. We must therefore be careful to ensure in the results presented that this assumption is justified. Here we consider the size of the response of the device as a function of frequency. Combining (9), (10), (13) and (17) we may show that

$$\Omega = (Z+\lambda)^{-1} A F_S \tag{49}$$

and so, since the maximum angle of excursion of the flap for a particular incident wave frequency may be expressed in terms of the complex angular velocity as $|\Theta| = |\Omega/\omega|$, we have

$$\left|\frac{\Theta}{H}\right| = \frac{|\Omega|}{H\omega} = \frac{|AF_S|}{|Z+\lambda|H\omega}, \tag{50}$$

the measure of the maximum displaced angle of the flap per unit height of incident wave.

B. Irregular Waves

In the results presented later we will consider the optimal device performance when subject to irregular waves. To do this we need to introduce a wave energy spectrum $E(T,\beta)$ which is used to represent a more realistic sea state. We choose the following form

$$E(T,\beta) = \phi_K(\omega) S_{BS}(T) D(\beta) \tag{51}$$

where $S_{BS}(T)$ denotes the Bretschneider Spectrum [7], designed to model seas over long fetches in deep water, $\phi_K(\omega)$ is an additional depth dependent factor of the form suggested

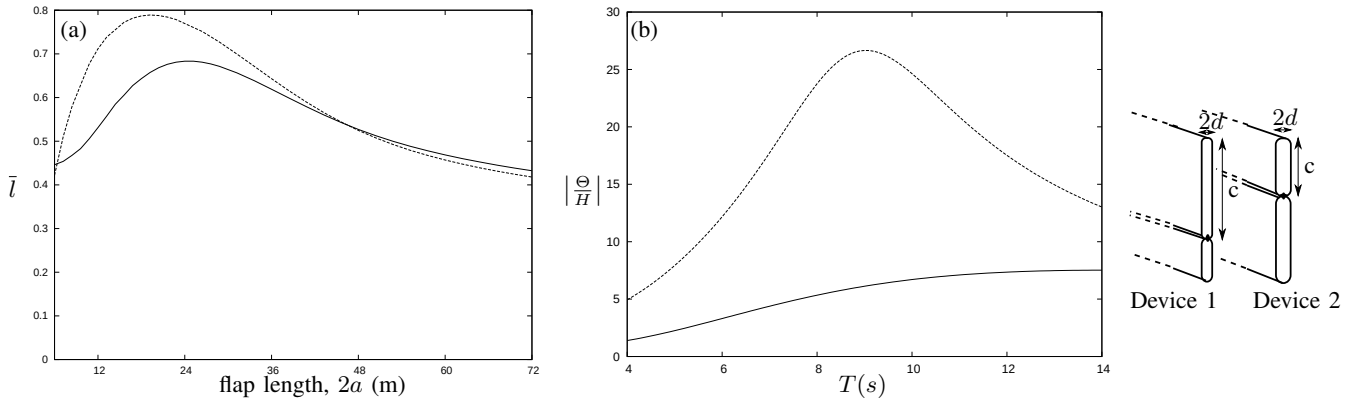

Figure 2. Variation of (a) mean capture factor $\bar{l}$ with flap length $2a$ in metres and (b) maximum angle of excursion per unit height of incident wave with wave period $T(s)$ along with scale diagrams of the devices. The solid line corresponds to device configuration 1 and the dashed line to device configuration 2. Optimal λ has been determined and used at each flap length in (a).

by [8] for the JONSWAP (Joint North Sea Wave Project) spectrum and

$$D(\beta) = \begin{cases} \frac{3}{\pi}(\cos(6\beta)+1) & \text{if } -\frac{\pi}{6} < \beta < \frac{\pi}{6} \\ 0 & \text{otherwise} \end{cases} \quad (52)$$

is used to model the directional spread of incident waves in the nearshore environment.

The mean incident wave power per unit crest length for this spectrum is given by

$$\overline{W}_{inc} = 2\pi\rho g \int_{-\frac{\pi}{6}}^{\frac{\pi}{6}} \int_0^\infty c_g(T) E(T,\beta) T^{-2}\, dT\, d\beta \quad (53)$$

whilst the average power absorbed by a wave surge converter is

$$\overline{W} = 2\pi\rho g \int_{-\frac{\pi}{6}}^{\frac{\pi}{6}} \int_0^\infty c_g(T) E(T,\beta) 2a\, \hat{l}(T,\beta) T^{-2}\, dT\, d\beta. \quad (54)$$

Here $c_g(T)$ denotes the finite depth group velocity, expressed as function of the wave period. Combining these expressions we can define a mean capture factor

$$\bar{l} = \frac{\overline{W}}{2a\overline{W}_{inc}}. \quad (55)$$

We will aim to maximise this quantity subject to some physical constraints and assumptions about the sea state.

We choose a model sea state with significant wave height $H_{\frac{1}{3}} = 2.83m$ and peak wave period $T_p = 9s$ as suggested by [9] consistent with an annual average power of approximately

$$W = \frac{\rho g^2 H_{\frac{1}{3}}^2 T_p}{64\pi} \simeq 30kW/m. \quad (56)$$

C. The physical parameters of the device

Having treated the flap as infinitely thin for the solution of the hydrodynamic problem, we now give the device a width $2d$ to enable us to specify its physical properties such as mass, moment of inertia and buoyancy torque. The flap is assumed to have mean density ρ_s and to extend from its pivot, located at a depth $z = -h + c$, to a non-zero depth $z = -h + b$. This gives a flap height of $(b-c)$m. The moment of inertia of the flap about the pivot is given by $I = \frac{1}{3}M_s((b-c)^2 + d^2)$ where $M_s = 4\rho_s d(b-c)a$ is the mass of the flap. The mass of water displaced by the flap is given by $M_w = 4\rho d(b-c)a$ where the fluid has density ρ and the constant of proportionality in the buoyancy torque is then $C = \frac{1}{2}M_w(1-s)g(b-c)$. Here $s = \rho_s/\rho = M_s/M_w$ denotes the specific gravity of the flap.

VI. Results

A. The Surface Piercing Flap

First we focus our attention on the numerical optimisation used to determine optimal device configuration for a full depth, surface piercing device. Optimal parameters were found by taking advantage of the high numerical efficiency of the solution method to embed the calculation of mean capture factor in a multi-dimensional numerical optimisation procedure. This was given as free parameters the flap width $2d$, flap length $2a$, hinge depth c, power take-off parameter λ and specific gravity s. Sensible bounds were set on the values these parameters could take and the depth of the water was fixed at $h = 12m$. The optimal parameters determined are shown in table I along with their corresponding mean capture factors $\bar{l}$.

Device	$2a$ (m)	$2d$ (m)	c (m)	s	λ	$\bar{l}$
1	24.6	1.9	8.4	0.15	7.54	0.684
2	19.2	2.4	5.0	0.15	2.02	0.789

TABLE I
OPTIMAL DEVICE PARAMETERS FOR TWO DEVICE CONFIGURATIONS ALONG WITH CORRESPONDING MEAN CAPTURE FACTORS.

The first row gives optimal values when the hinge height and flap width were fixed at values representative of the Oyster [1], termed device 1. In this case the specific gravity selects its lower bound, which was set at 0.15 whilst the optimal device length was found to be 24.6m, commensurate with the second generation 'Oyster 800' device. In the second row all

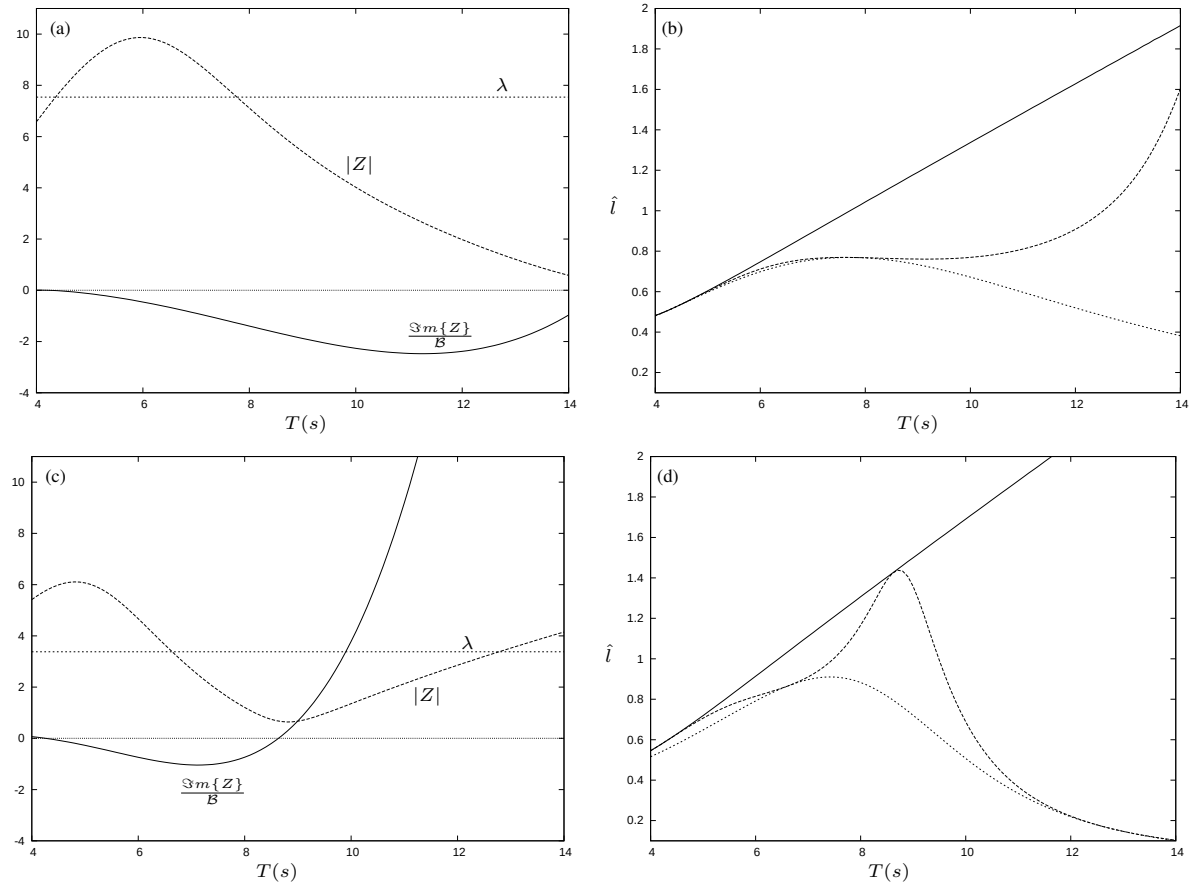

Figure 3. Variation of: (a) $|Z|$ and $\Im m\{Z\}/\mathcal{B}$, and (b) capture factors $\hat{l}_{max}$, $\hat{l}_{opt}$ and $\hat{l}$ with period T in seconds for optimal flap parameters, shown in table I. The first two figures show results for device configuration 1 and the second two those for device configuration 2.

parameters were allowed to vary. This configuration favours a shorter flap with a higher hinge point than the Oyster and is termed device 2.

Device length is critical to performance and this is highlighted in Figure 2(a). The variation of mean capture factor $\bar{l}$ with flap length $2a$ is shown for both device configurations, the optimal value of λ having been determined for each length. A clear peak may be seen in both cases with the peak for the second device configuration being skewed further to the left than that of device 1 suggesting a shorter optimal flap length of 19.2m when the hinge is positioned higher on the device. The maximum mean capture factor is also higher for device 2 than for device 1 demonstrating a greater power absorption potential. However, the 15% increase in $\bar{l}$ obtained with a higher hinge position is offset by a significant increase in the amplitude of the flap oscillations. In figure 2(b) the flap excursion per unit height of incident wave is shown as a function of incident wave period for both device 1 and device 2. The peak in the flap excursion for device 2 is suggestive of resonance at $T \simeq 9s$. The problem being that this also results in a peak flap excursion of 26.5°, motion of this magnitude could be poorly approximated by a linearised theory. Meanwhile, for device 1 (where parameters have been chosen to be representative of the Oyster) we see a maximum flap excursion per incident wave height of just 7°, confirming linearised theory is an appropriate approximation in this case.

With the optimal parameters determined we turn our attention to the components of optimisation, considering the single-frequency capture factor of the flap as a measure of its performance. This is given by (15) to be

$$\hat{l} = \hat{l}_{max} \frac{2\mathcal{B}}{\mathcal{B} + |Z|} \left(1 - \frac{(\lambda - |Z|)^2}{|\lambda + Z|^2} \right) \tag{57}$$

where

$$\hat{l}_{max} = \frac{1}{2a} \frac{|AF_S|^2}{8\mathcal{B}W_{inc}} = \frac{2\pi |F_S(\beta)|^2}{2ka \int_0^{2\pi} |F_S(\theta)|^2 \, d\theta} \tag{58}$$

and the second equality results after use of the Haskind relation in three dimensions (e.g. [10]) with the exciting force having been expressed as a function of incident wave direction, β. Thus, there are three main ingredients in the determination of the capture factor. The first (58) sets $\hat{l}_{max}$ and is decided by the geometry of the wave absorber. This depends on scattering of waves by the fixed absorber and is optimised by a highly directional force profile as a function of wave angle. The flap

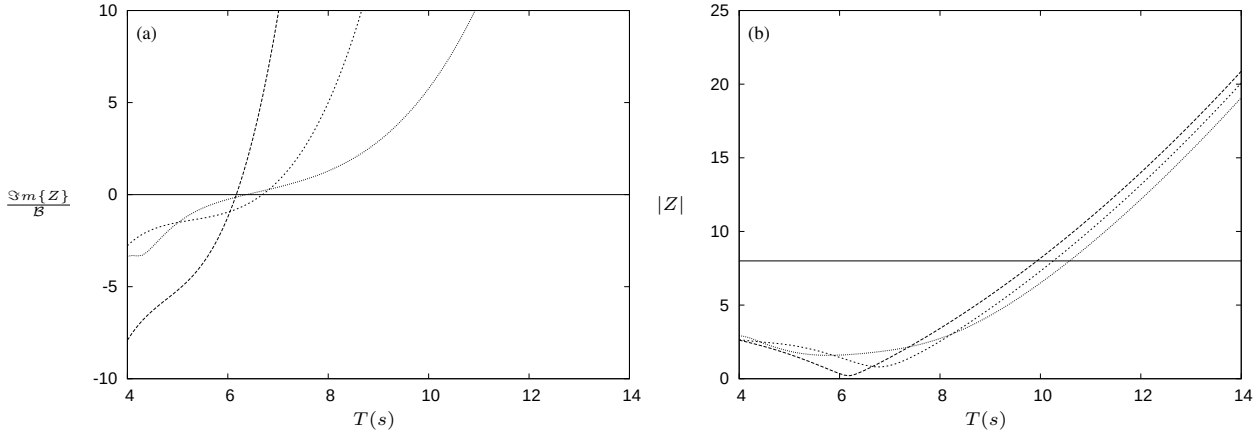

Figure 4. Variation of: (a) $\Im m\{Z\}/\mathcal{B}$ and (b) $|Z|$ and λ and (c) $|\Theta/H|$ with incident wave period T. The proportion of the depth taken up by the flap is fixed at $b/h = 0.9$ whilst the curves of decreasing dash length represent $a/h = 0.5, 1.0$ and 2.0 respectively. The solid lines show: (a) zero and (b) $\lambda = 8$.

offers this feature. The second factor multiplies $\hat{l}_{max}$ to set $\hat{l}_{opt}$ and depends on hydrodynamic coefficients,

$$\frac{2\mathcal{B}}{\mathcal{B}+|Z|} = \frac{2}{1+(1+(\Im m\{Z\}/\mathcal{B})^2)^{1/2}}. \tag{59}$$

The key to optimising this is making the factor $\Im m\{Z\}/\mathcal{B}$ as small as possible over a range of periods so that $\hat{l}_{opt}$ remains close to $\hat{l}_{max}$. In fact, resonance occurs when this quantity vanishes since when this is the case $\omega^2(\mathcal{A}+I) = C$ and the moment of inertia, plus added inertia, is balanced by the restoring forces due to buoyancy. An illustration of the key role this factor plays in device performance is shown in figure 3 for the optimal parameters given in table I. In figure 3(a) we see that despite not achieving true resonance device 1 is near resonant across a wide range of incident wave periods. This behaviour is central to the broad-banded success of the Oyster Device. Meanwhile, in figure 3(c) we notice that the natural resonant period of device 2 does fall within the range of interest. This reduction of the resonant period is due to a combination of reducing device length, increasing the width and raising the hinge position and tallies with the numerical findings of [3] and [2] where it is suggested that shorter, wider devices have lower resonant periods. Again this quantity remains small across the full range, especially for lower wave periods where the energy in the nearshore spectrum is focused.

It is through the final component that the power take-off parameter plays a part. Optimal tuning requires $\lambda = |Z|$ and results in $\hat{l}$ attaining $\hat{l}_{opt}$. Generally, λ is constant and so we are looking for $|Z|$ to be relatively flat. λ may then be fixed at a value determined by the weighted average of $|Z|$ over a real sea spectrum. Here λ has been determined to be optimal for the real sea spectrum described in §*V-B*. The explanation given above suggests mathematical reasons for the broad-banded success of flap-type converters as a wave energy design solution. Optimising the performance of the device involves finely tuning these three components so that each is optimised in unison.

B. Fully Submerged Flap

We now investigate the impact on the performance characteristics when the flap is fully submerged. The components of optimisation associated with a fixed proportion of the depth $b/h = 0.9$ and varying flap lengths $a/h = 0.5, 1.0$ and 2.0 are shown in Figure 4. This corresponds with the best results, shown in the top row of Figure 5, where actual, optimum and maximum capture factors are plotted for a range of flap lengths. We will come back to the maximum capture factor shortly. First, we consider the factors which play a role in resonance and tuning. Figure 4a) shows $\Im m\{Z\}/\mathcal{B}$, which determines resonance. We see that whilst in all cases the natural resonant period falls within the range of interest, this component becomes large quickly leading to a narrow resonant peak. The lower natural resonant periods seen here for all device lengths are similar to that seen in Figure 3c) and are due to shortening the flap height; in §*VI-A* by raising the hinge position and here by submerging the flap to varying degrees.

The other factor which plays a role is $|Z|$, which as before we want to be relatively flat. This condition is closest to being met for short devices, however in all cases $|Z|$ undergoes larger deviations from its mean value than for the full depth device with parameters representative of the Oyster. The theoretical maximum, which forms an upper bound, is at its highest when $a/h = 0.5$ and the flap is short. However, this also corresponds to a narrower resonant peak than that seen for longer devices. Whilst an improvement in the actual capture factors over those plotted in Figure 5 may be achieved through optimal tuning, this unfortunate combination of characteristics leads to a narrow peak and actual capture factors being limited to a mean value of about 0.3. By comparison, when optimally configured, the results for a surface piercing device are close to 0.7 for a broad range of periods as seen in §*VI-A*. It is not obvious that such a deterioration in performance should be seen as a result of complete submersion. Indeed, high capture factors are maintained for some devices and this is the case for the fully submerged device of [11] for example.

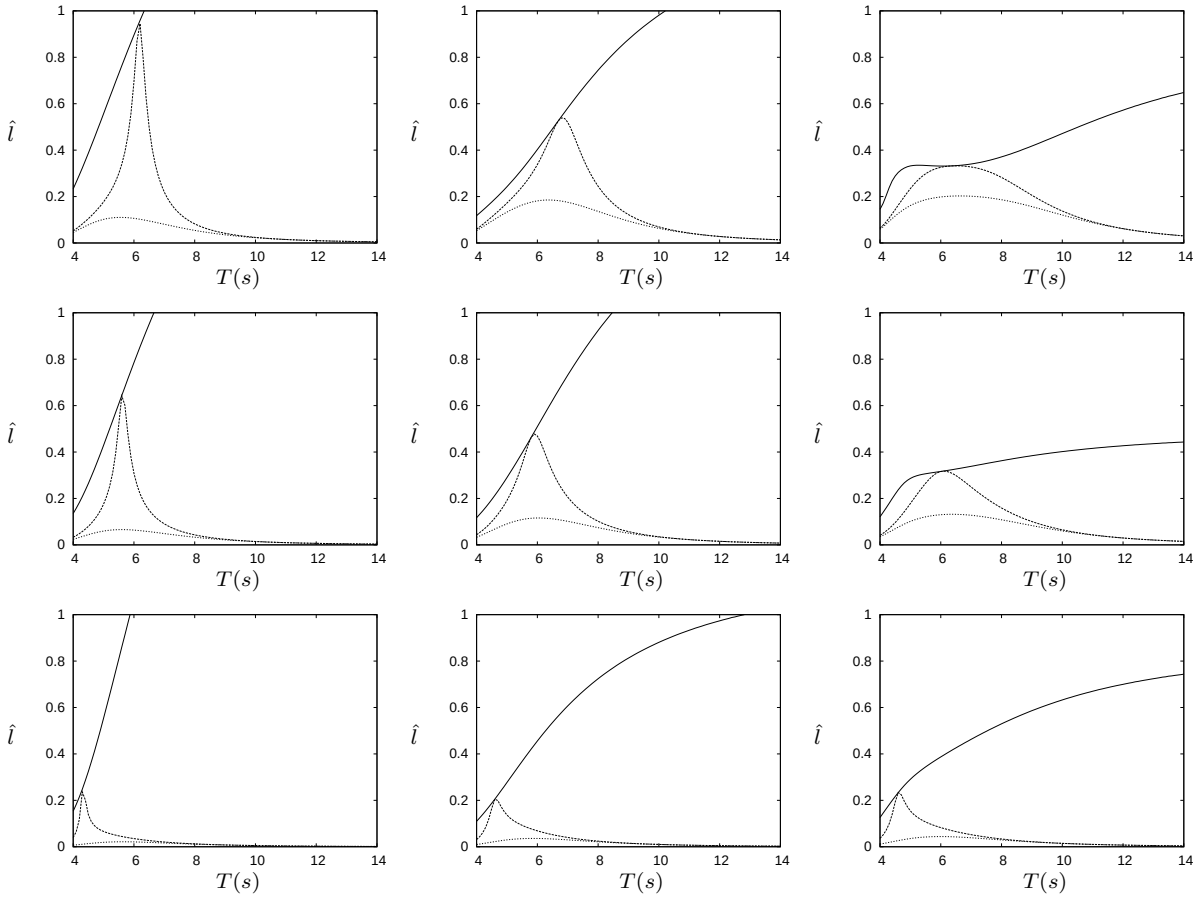

Figure 5. Capture factors plotted as a function of wave period $T(s)$ for flaps of various lengths and heights in water of fixed depth $h = 12m$. The hinge height is fixed at $c = 0.2h$ and the power take-off at $\lambda = 8$. The rows show results for $b/h = 0.9, 0.8$ and 0.6 respectively, moving down the page, whilst the columns show results for $a/h = 0.5, 1.0$ and 2.0, from left to right. The dotted, dashed and solid curves show $\hat{l}$, $\hat{l}_{opt}$ and $\hat{l}_{max}$ respectively.

VII. Conclusions

An analytical approach to calculations assessing the efficacy of three-dimensional flap-type wave energy converters has been taken. The natural resonant period of the Oyster device is outside the range of interest at around 20s and so a lower value would be desirable. We have seen in the results presented that this may be achieved through shortening the height of the flap; either by raising the hinge position or by fully submerging the device. Full submersion of the device has the added advantage of increased survivability away from the adverse effects of the surface region. However, the reduction of the resonant period to within the range of interest is combined with weaker performance characteristics outside the resonant peak than seen for parameters representative of the Oyster and these losses appear to be too great to make a fully submerged device a viable solution.

Acknowledgment

I.F. Noad wishes to acknowledge the receipt of a University of Bristol Postgraduate Research Scholarship.

References

[1] Aquamarine Power Ltd, http://www.aquamarinepower.com/, 2014, accessed: August 2014.

[2] T. Whittaker and M. Folley, "Nearshore oscillating wave surge converters and the development of oyster," *Phil Trans R Soc A: Math Phys and Eng Sci*, vol. 370, no. 1959, pp. 345–364, 2012.

[3] M. Folley, T. Whittaker, and J. Van't Hoff, "The design of small seabed-mounted bottom-hinged wave energy converters," in *Proceedings of the 7th European Wave and Tidal Energy Conference, Porto, Portugal*, 2007.

[4] E. Renzi and F. Dias, "Hydrodynamics of the oscillating wave surge converter in the open ocean," *Eur J Mech-B/Fluids*, vol. 41, pp. 1–10, 2013.

[5] I. F. Noad and R. Porter, "Optimisation of arrays of flap-type oscillating wave surge converters," *App Ocean Res*, vol. 50, pp. 237–253, 2015.

[6] D. V. Evans and R. Porter, "Wave energy extraction by coupled resonant absorbers," *Philos Trans R Soc A: Math Phys Eng Sci*, vol. 370, no. 1959, pp. 315–344, 2012.

[7] C. L. Bretschneider, "Wave variability and wave spectra for wind-generated gravity waves," DTIC Document, Tech. Rep., 1959.

[8] E. Bouws, H. Günther, W. Rosenthal, and C. L. Vincent, "Similarity of the wind wave spectrum in finite depth water: 1. spectral form," *J Geophys Res: Oceans (1978–2012)*, vol. 90, no. C1, pp. 975–986, 1985.

[9] J. Falnes, "A review of wave-energy extraction," *Mar Struct*, vol. 20, no. 4, pp. 185–201, 2007.

[10] J. V. Wehausen and E. V. Laitone, *Surface waves*. Springer, 1960.

[11] S. Crowley, R. Porter, and D. Evans, "A submerged cylinder wave energy converter with internal sloshing power take off," *Eur J Mech-B/Fluids*, vol. 47, pp. 108–123, 2014.